

# Autosomal dominant retinitis pigmentosa with incomplete penetrance due to an intronic mutation of the *PRPF31* gene

Tahleel Ali-Nasser,<sup>1</sup> Shiri Zayit-Soudry,<sup>1,2,3</sup> Eyal Banin,<sup>4</sup> Dror Sharon,<sup>4</sup> Tamar Ben-Yosef<sup>1</sup>

<sup>1</sup>Ruth & Bruce Rappaport Faculty of Medicine, Technion-Israel Institute of Technology, Haifa, Israel; <sup>2</sup>Department of Ophthalmology, Rambam Health Care Campus, Haifa, Israel; <sup>3</sup>Clinical Research Institute at Rambam, Rambam Health Care Campus, Haifa, Israel; <sup>4</sup>Department of Ophthalmology, Hadassah-Hebrew University Medical Center, Jerusalem, Israel

**Purpose:** To identify the molecular mechanisms of the development of autosomal dominant retinitis pigmentosa (adRP) with incomplete penetrance in an Israeli Muslim Arab family.

**Methods:** Two patients with adRP underwent a detailed ophthalmic evaluation, including funduscopy examination, visual field testing, optical coherence tomography, and electroretinography. Genetic analysis was performed using a combination of whole exome sequencing (WES) and Sanger sequencing. The pathogenicity of the identified intronic variant was evaluated *in silico* using several web-based tools, *in vitro* using a minigene-based assay, and *in vivo* using reverse transcription PCR analysis of lymphocyte-derived RNA. The relative abundance of alternatively spliced transcripts was evaluated using amplicon-based next-generation sequencing. The relative expression levels of *PRPF31* and *CNOT3* were measured using quantitative PCR (qPCR) analysis.

**Results:** The two patients recruited in this study had childhood-onset RP, with night blindness as the initial symptom, followed by concentric restriction of the visual field. The funduscopy findings included narrowed retinal blood vessels and peripheral bone spicule pigmentation. By the third decade of life, the full-field electroretinography findings had been remarkably attenuated. In these patients, we identified a novel heterozygous intronic variant at position +5 of *PRPF31* intron 11 (c.1146+5G>T). The same variant was also detected in one asymptomatic family member. Through *in silico* analysis, the variant was predicted to alter the splicing of intron 11. An *in vitro* splicing assay and a reverse transcription PCR analysis of lymphocyte-derived RNA revealed that the mutant allele yielded mainly a shorter transcript in which exon 11 was skipped. The skipping of exon 11 was expected to cause a frameshift and an aberrant truncated protein (p.Tyr359Serfs\*29). The qPCR analysis revealed reduced *PRPF31* expression levels in the mutation carriers, without a significant difference between the affected patient and his asymptomatic brother. We evaluated several factors that have been suggested to correlate with non-penetrance of *PRPF31* mutations, including the number of cis-acting MSR1 elements adjacent to the *PRPF31* core promoter, *CNOT3* expression level, and *CNOT3* rs4806718 single-nucleotide polymorphism. None of these factors correlated with non-penetrance in the family in this study.

**Conclusions:** We report a novel intronic mutation in *PRPF31* underlying adRP. This report expands the spectrum of pathogenic mutations in *PRPF31* and further demonstrates the importance of intronic mutations. Moreover, it demonstrates the phenomenon of incomplete penetrance previously associated with *PRPF31* mutations. The fact that the non-penetrance in the family in this study could not be explained by any of the known mechanisms suggests the possible contribution of a novel modifier of *PRPF31* penetrance.

Retinitis pigmentosa (RP), having a worldwide prevalence of approximately 1 in 4,000 individuals, is the most common form of inherited retinal dystrophy (IRD). In RP (also known as rod-cone degeneration), rod photoreceptors are initially more severely affected than cone photoreceptors; thus, the first clinical symptoms are usually night blindness and gradual restriction of the visual field. Ophthalmologic findings include characteristic pigmentation of the mid-peripheral retina, attenuation of retinal arterioles, and optic disc pallor [1]. RP is one of the most genetically heterogeneous conditions in humans and can be inherited as autosomal

dominant (AD), autosomal recessive, or X-linked. To date, more than 90 genes have been implicated in nonsyndromic RP, of which at least 31 are associated with an AD mode of inheritance (RetNet [Retinal Information Network]).

Pre-mRNA processing factor 31 (PRPF31) is a ubiquitous pre-mRNA splicing factor that is part of the U4/U6\*U5 tri-small nuclear ribonucleoprotein complex of the spliceosome. The heterozygous mutations of *PRPF31* are the major causes of adRP (RP11; OMIM No. 600138) [2], accounting for 6%–11% of cases in various populations [3]. Most of more than 130 *PRPF31* mutations reported to date are presumed loss-of-function variants, including frameshift, splice site, and nonsense or large-scale insertions or deletions [3]. Genotype-phenotype correlation was observed between the mutation type and age of onset. The lowest age of onset

Correspondence to: Tamar Ben-Yosef, Rappaport Faculty of Medicine, Technion, P.O. Box 9649, Bat Galim, Haifa 31096, Israel; Phone: 972-4-829-5228; FAX: 972-4-829-5225; email: benyosef@technion.ac.il

is associated with nonsense and frameshift variants, followed by large deletions or splice variants. In-frame duplications, insertions, or missense variants show the highest median age of onset [3].

The abundance of loss-of-function mutations in patients with *RP11*, including complete gene deletions, has led to a consensus view that haploinsufficiency is the disease mechanism in this form of RP [4]. An interesting observation (although not statistically significant) is that patients with large-scale deletions (partial or complete gene loss) have a higher age of diagnosis than patients with other mutation types [3]. On the basis of this observation, it could be postulated that an element of dominant negative effect is involved in cases of nonsense, frameshift, indel, in-frame, and missense variants compared with large deletions. This is further supported by recent works that have shown that at least some *PRPF31* mutations are associated with a combined haploinsufficiency and dominant-negative disease mechanism [3,5].

A hallmark of *PRPF31*-associated RP is incomplete penetrance; that is, obligate carriers may be totally asymptomatic but can still pass pathogenic mutations to their offspring. This phenomenon has been reported worldwide in multiple families harboring various *PRPF31* mutations [3]. A major determinant of *PRPF31* mutation penetrance is the expression level of the nonmutant *PRPF31* allele. High expressors of this allele compensate for the deficiency of the mutant allele and have normal vision, whereas low expressors develop RP due to an insufficient amount of functional *PRPF31* protein [6]. Wild-type (wt) *PRPF31* transcript abundance is a highly variable and heritable characteristic [7]. Several factors contributing to the varied expression levels have been proposed, including expression quantitative trait loci (eQTLs) on chromosome 14, in trans with *PRPF31* [7]; the variable expression level of *CNOT3*, encoding a subunit of the Ccr4-not transcription complex, which binds to and represses the transcription of the *PRPF31* promoter [8,9]; and the number of cis-acting minisatellite repeat (MSR1) elements adjacent to the *PRPF31* core promoter, which determines the level of *PRPF31* transcriptional repression [10,11]. Based on these observations, the mechanism of incomplete penetrance in RP11 has been described as “variant haploinsufficiency,” in which the existence and/or the severity of disease depends on the type of the mutant allele inherited [3], and the levels at which this allele and the wt allele are expressed [4]. Herein, we describe a family segregating adRP with incomplete penetrance due to an intronic mutation of the *PRPF31* gene.

## METHODS

**Patients:** In this study, the tenets of the Declaration of Helsinki were followed. This study was approved by the institutional review boards of the participating medical centers, and written informed consent was obtained from all participants. Ophthalmic examination included measurement of the best-corrected visual acuity, visual field testing, slit-lamp biomicroscopy of the anterior segment and ophthalmoscopic examination after pharmacological pupillary dilatation, spectral-domain optical coherence tomography (SD-OCT), and full field electroretinography (ff-ERG).

**DNA analyses:** Genomic DNA was extracted from venous blood samples using a high-salt solution in accordance with the standard protocol [12]. Whole exome sequencing (WES) of Subject II:1 was performed at 3billion (Seoul, South Korea) using xGen Exome Research Panel v2 (Integrated DNA Technologies, Coralville, IA) and Novaseq 6000 (Illumina, San Diego, CA). Sequence reads were aligned to the reference human genome (GRCh37/hg19). Variants were called via the [Franklin web-based pipeline](#) by Genoox. The genotyping of family members was performed using PCR amplification of the relevant DNA segments with specific primers (Appendix 1), followed by Sanger sequencing.

**In vitro splicing analysis:** An in vitro evaluation was performed using a minigene-based assay. To create wt and mutant minigene constructs, a 1,028-bp DNA fragment harboring *PRPF31* exons 10, 11, and 12, and the introns between them was PCR amplified from the genomic DNA of the patient (Appendix 1). Fragments harboring either the wt or mutant allele were inserted in the pCMV-Script mammalian expression vector (Stratagene, La Jolla, CA). Constructs were transfected into COS-7 cells using the jetPEI transfection reagent (Polyplus-transfection, Illkirch, France). Cells were cultured in a DMEM culture medium supplemented with 10% fetal bovine serum (Biologic Industries, Beit Ha'emek, Israel) and maintained at 37 °C and 5% CO<sub>2</sub>. Twenty-four hours after transfection, total RNA was extracted from the cells using TRI Reagent (Sigma-Aldrich, St Louis, MO) and treated with RQ1 RNase-free DNase (Promega, Madison, WI). Reverse transcription was performed with 1 µg of DNase-treated total RNA in a 20-µl reaction volume using 200 U of M-MLV reverse transcriptase and 100 ng of random primers (Stratagene). Two microliters of cDNA were subjected to PCR amplification with a forward primer in exon 10 and a reverse primer in the vector (T7; Appendix 1). The PCR products were subcloned into the pGEM-Teasy vector (Promega), and several independent clones of each product were sequenced. The COS-7 cells used for this experiment were authenticated by genotyping 4 STR markers (D17S1304, D5S1467,

D4S2408, and D19S245). Genotyping was performed with PCR amplification of each STR and direct sequencing, as described by Almeida et al. [13]. The results (in terms of the repeat number for each STR) were compatible with those described for COS-7 cells (data not shown) [13].

*In vivo splicing analysis:* For the in vivo evaluation, total RNA was isolated from fresh blood lymphocytes using TRI Reagent, treated with RQ1 RNase-free DNase, and reverse transcribed as described earlier. PCR amplification was performed with forward and reverse primers in exons 10 and 12, respectively (Appendix 1). For sequencing, the PCR products were cloned into the pGEM-Teasy vector (Promega).

*Amplicon-based next-generation sequencing:* Amplicon-based next-generation sequencing (NGS) was performed at the Technion Genomics Center. Lymphocyte-derived RT-PCR products (described in the previous section, “In vivo splicing analysis”) were prepared for NGS according to the “16S Library Preparation protocol” by Illumina. This included PCR product purification, barcode attachment, and second purification of the final libraries. The concentration of each library was measured using the Qubit dsDNA HS Assay Kit (Life Technologies, Thermo Fisher Scientific, Waltham, MA), and the size was determined using TapeStation 4200 with the High Sensitivity D1000 Kit (Agilent, Santa Clara, CA). All libraries were mixed into a single tube with equal molarity. DNaseq data were generated on Illumina MiSeq as 150 paired-end reads. Demultiplexing was executed using bcl2fastq version v2.20.0.422 software (Illumina), with one barcode mismatch allowed and a minimum trimmed read length of 35. Quality control was assessed using Fastqc (v0.11.8), 150-bp paired-end reads were trimmed for adapters, low-quality 3', and a minimum length of 30 using CUTADAPT (v1.10). Next, the reads were simultaneously mapped to two references: long.fasta, including exons 10, 11, and 12, and short.fasta, including exons 10 and 12. Mapping was performed using the BBSplit tool from BBTools (version 38.95) with default parameters, where ambiguous reads were binned to the first best reference.

*Quantitative PCR:* cDNA was synthesized using the qPCRBIO High-Quality cDNA Synthesis Kit (PCR Biosystems, London, UK). qPCR reactions were prepared using 2X qPCRBIO Fast qPCR SyGreen Blue Mix (PCR Biosystems, London, UK) and performed using the QuantStudio3 Real-Time PCR System (Applied Biosystems, Thermo Fisher Scientific). Data were analyzed using the  $\Delta\Delta C_T$  method. Gene expression values were normalized against the *GAPDH* expression level. The primer sequences are presented in Appendix 1.

## RESULTS

*Clinical findings from the affected individuals:* TB209 is a Muslim Arab family from Northern Israel, segregating adRP. The affected individuals (subjects II:1 and III:1; Figure 1A) were a mother and her son, aged 54 and 32 years old at the time of the last follow-up, respectively. Both reported childhood-onset night blindness as the initial symptom, which was associated with subjectively worsening dark and light adaptation, followed by a progressive, concentric restriction of the visual field. Subject II:1 also complained of decreasing visual acuity in both eyes several years prior. A posterior subcapsular cataract was present in both eyes of both subjects. The ophthalmoscopic findings included pallor of the optic nerve head, cellophane macular reflex, and narrowed retinal arteries with perivascular and midperipheral bone spicule pigmentation of the retina. Macular imaging using SD-OCT revealed loss of the outer nuclear layer (ONL) and inner segment ellipsoid zone (EZ) band, with preservation of this landmark only in the foveal center in Subject II:1. This patient also had focal vitreomacular traction with cystoid macular changes mainly in the right eye. In Subject III:1, the SD-OCT imaging revealed relative preservation of the EZ and ONL in the fovea, whereas ff-ERG at the age of 29 years was attenuated to a non-measurable level (Table 1 and Figure 2).

*Identification of a *PRPF31* intronic mutation using WES:* To identify the genetic cause of the disease in family TB209, WES analysis (including copy number variation detection) was performed on a DNA sample from Subject II:1. A heterozygous variant at position +5 of intron 11 in the *PRPF31* gene (NM\_015629) was identified (c.1146+5G>T; IVS11+5G>T; Figure 1B, C). Through in silico analysis, this variant was predicted to alter the splicing of intron 11 (Table 2). The same variant appeared to be heterozygous in Subject III:1 (affected) and in his unaffected brother (Subject III:3; Figure 1A). This novel variant has never been reported in patients with IRD (neither in the literature nor in ClinVar); is not registered in public databases, including the Genome Aggregation Database, Trans-Omics for Precision Medicine (TOPMed) Bravo, The Greater Middle East (GME) Variome, and the Exome Sequencing Project (ESP) 6500; and is absent in more than 1000 exomes of Israeli patients with IRD.

*Effect of c.1146+5G>T on splicing:* We initially used an in vitro splicing assay approach that enabled us to examine each allele (wt vs. mutant) separately and evaluate the effect of c.1146+5G>T on splicing. For this purpose, we created two minigene constructs (wt and mutant) harboring *PRPF31* exons 10 to 12 and the introns between them, downstream of a CMV promoter. Constructs were transfected into COS-7 cells, followed by RNA extraction and RT-PCR analysis.

To specifically detect *PRPF31* transcripts obtained from the minigene constructs (and not from the endogenously expressed gene), we performed PCR amplification with a forward primer derived from exon 10 and a reverse primer derived from the expression vector (Figure 3A). The wt

construct yielded both the expected product harboring exons 10, 11, and 12 (exon 11+) and a shorter product in which exon 11 was skipped (exon 11-). The mutant construct mainly yielded the shorter product (exon 11-; Figure 3A,B). The

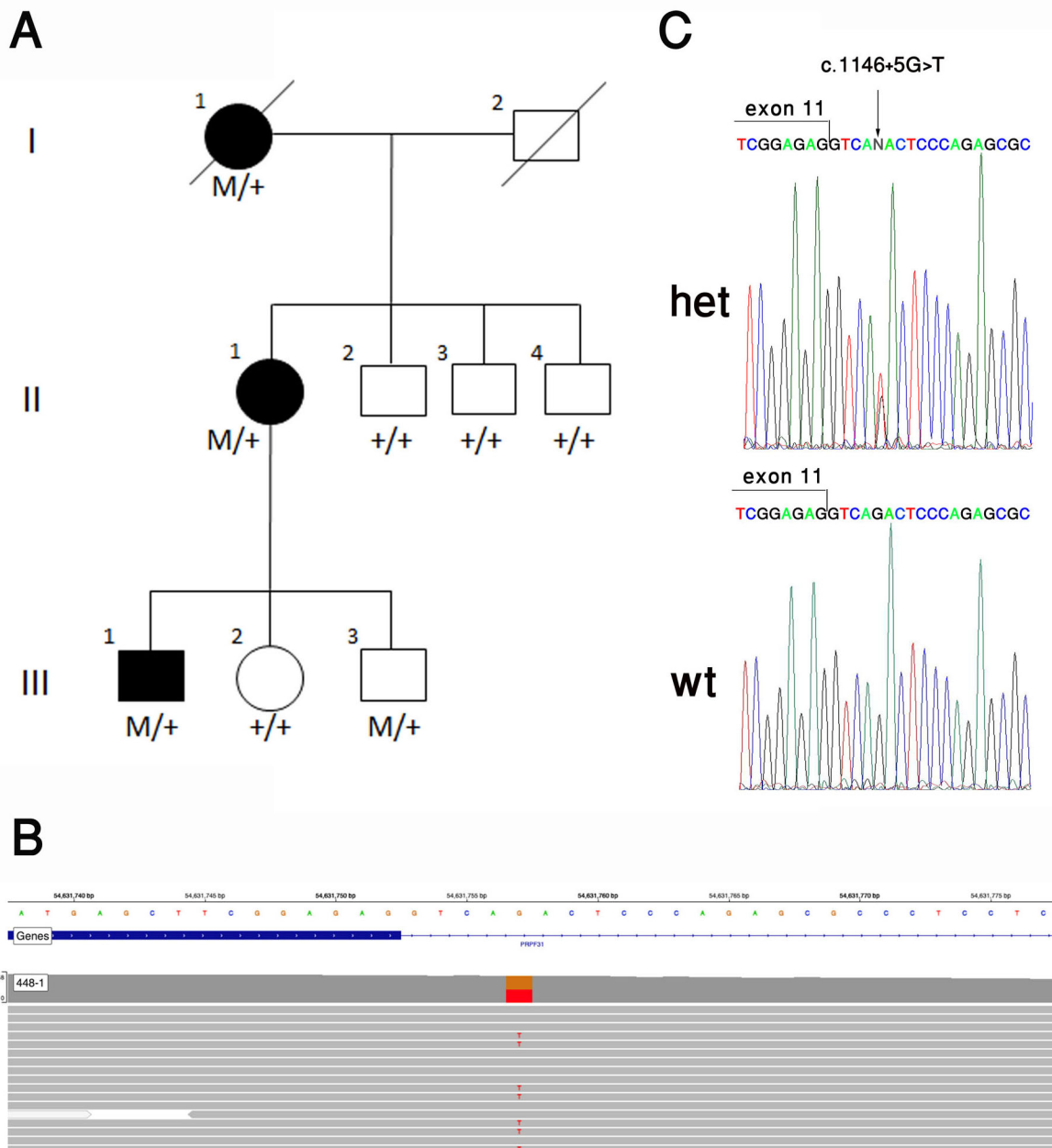


Figure 1. Pedigree and mutation analysis. **A:** A Muslim Arab family segregating adRP due to the c.1146+5G>T mutation in *PRPF31*. Filled symbols represent affected individuals, whereas clear symbols represent unaffected individuals. The genotypes of the family members are indicated below them (+, wt; M, mutant). **B:** Integrative Genomics Viewer (IGV) visualization of the boundary between *PRPF31* exon 11 and intron 11 in Subject II:1, showing a heterozygous G>T transversion at position 54,631,757 of chromosome 19 (GRCh37/hg19). **C:** Nucleotide sequence traces of the boundary between *PRPF31* exon 11 and intron 11 in a non-carrier individual (wt) and an affected individual heterozygous for the c.1146+5G>T mutant allele (het).

TABLE 1. CLINICAL FINDINGS IN PATIENTS FROM FAMILY TB209.

Patient number (Gender)	Onset	Age at diagnostic exam	Eye	Best corrected visual acuity	Fundus	Visual field	ff-ERG			Additional ocular findings
							LA Single flash	LA flicker (30Hz) <sup>a</sup> Amp IT (µV; mS)	DA	
II:1 (F)	Childhood	46y	RE	6/7			SR (BE)	23	NR (BE)	
			LE	6/9.5				43.8		
		54y	RE	6/15	Peripheral bone spicule pigmentation, attenuated veins (BE)	Concentric restriction (BE)				nuclear sclerosis (BE), posterior subcapsular cataract (BE)
			LE	6/15						
III:1 (M)	Childhood	29y	RE	6/6	Abnormal macular reflex, peripheral bone spicule pigmentation (BE)	Concentric restriction (BE)	NR (BE)	NR (BE)	NR (BE)	posterior subcapsular cataract (BE)
			LE	6/6						

<sup>a</sup> Light-adapted cone flicker amplitude (Amp., in µV, normal 60–144 µV) and implicit time (IT, in ms, normal 27–33 ms). F: female, M: male, y: years, RE: right eye, LE: left eye, BE: both eyes, ff-ERG: full-field electroretinogram, LA: light adapted (photopic), DA: dark adapted (scotopic), NR: non-recordable, SR: severely reduced.

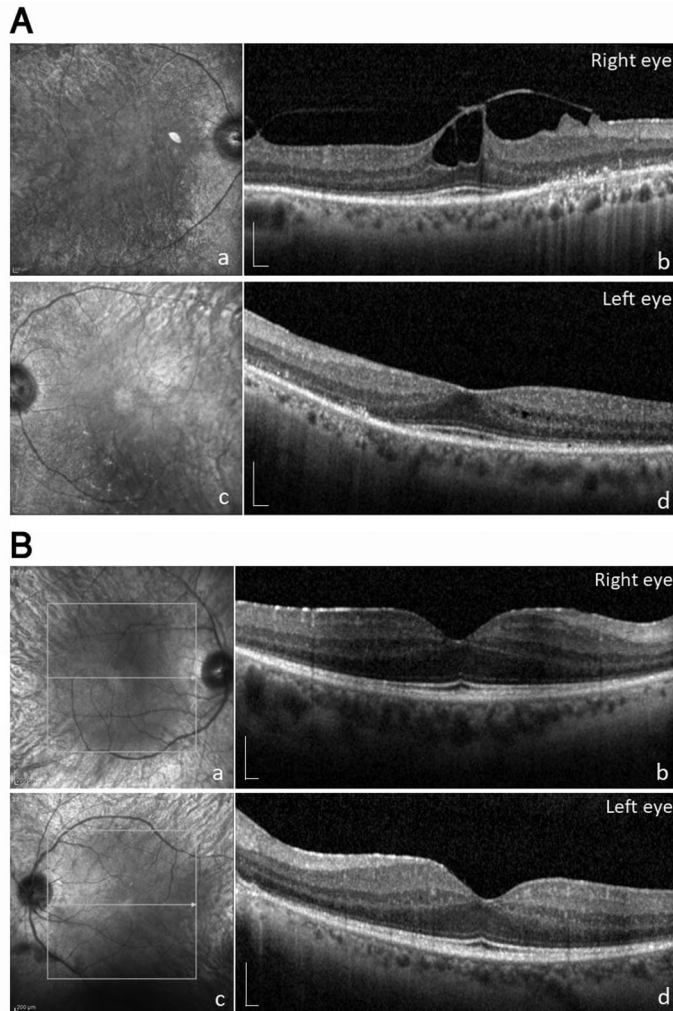


Figure 2. Clinical images of subjects II:1 and III:1. **A:** Clinical image of Subject II:1, showing retinal manifestations of outer retinal degeneration. The infrared scanning laser ophthalmoscopy (SLO-IR; a, c) and spectral-domain optical coherence tomography (SD-OCT; b, d) images of each eye show a perifoveal ellipsoid zone and outer nuclear layer loss, with preservation of these layers in the foveal center. Focal vitreomacular traction with distortion of the foveal contour can be observed in the right eye, whereas subtle cystic changes can be observed in the inner nuclear layer temporal to the fovea in the left eye. **B:** Macular image of Subject III:1. The infrared SLO-IR (a, c) and SD-OCT images (b, d) show preservation of the perifoveal ellipsoid zone and outer nuclear layer in the fovea, with perifoveal thinning of these structures in each eye. Calibration bars: 200 μm.

skipping of exon 11 was expected to cause a frameshift that yields an aberrant truncated protein (p.Tyr359Serfs\*29).

To evaluate the effect of c.1146+5G>T on splicing *in vivo*, we performed an RT-PCR analysis of leukocyte-derived RNA samples for all available family members, with primers located in exons 10 and 12. As expected, exon 11+ transcripts were detected in all tested individuals. Exon 11- transcripts were mainly detected in the individuals heterozygous for the c.1146+5G>T allele, although faint products could also be observed in the wt individuals (Figure 4A). To quantify the

amount of exon 11+ relative to that of exon 11- transcripts in the wt and heterozygous individuals, we applied amplicon-based NGS to the RT-PCR products of family members. The quantitative analysis of the NGS results confirmed that skipping of exon 11 occurred in both the wt and mutant individuals. Exon 11- reads composed 2%–5% of all unique reads in the wt individuals and 8%–10% in the individuals heterozygous for the c.1146+5G>T allele (Figure 4B, C).

*Evaluation of the molecular mechanism of the reduced penetrance of the c.1146+5G>T mutation:* As mentioned earlier, Subject III:3 was heterozygous for the c.1146+5G>T mutation. The clinical data of this individual were not available, but at the age of 32 years, he subjectively reported good vision and indicated that he was examined by an ophthalmologist, with no significant findings. Considering that both his mother and brother experienced onset of night blindness in childhood and that his brother's ff-ERG was non-recordable at the age of 29

TABLE 2. IN SILICO ANALYSIS OF THE EFFECT OF *PRPF31* c.1146+5G>T ON SPLICING.

Prediction tool	Prediction	Score (0–1)
<a href="#">dbscSNV Ada</a> [12]	Deleterious	1
Random Forest (RF) [13]	Deleterious	0.95
<a href="#">SpliceAI</a> [14]	Splice-Altering (low)	0.39

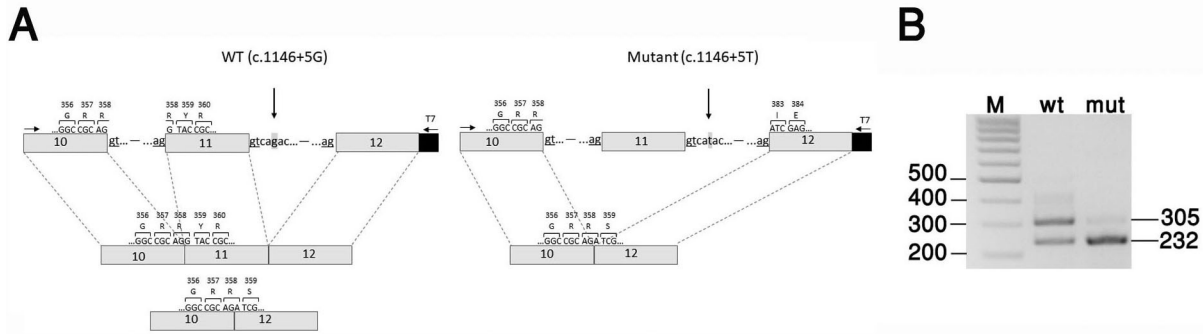


Figure 3. Evaluation of the effect of *PRPF31* c.1146+5G>T on splicing in vitro. **A, B:** Minigene constructs and products obtained in the in vitro splicing assay. Shown is a schematic representation of the constructs (**A**), which include *PRPF31* exons 10, 11, and 12 (represented by boxes) and the introns between them. Either G (wt) or T (mutant) is present at position +5 of intron 11. The locations of the primers used for the RT-PCR analysis are also shown (indicated by arrows). Constructs were transfected into COS-7 cells, followed by RNA extraction and RT-PCR analysis (**B**). cDNA derived from the wild-type (wt) construct yielded two splice products: one harboring exons 10, 11, and 12 and the other showing the skipping of exon 11. cDNA derived from the mutant construct mainly yielded the splice product lacking exon 11. wt, mutant; M, size marker.

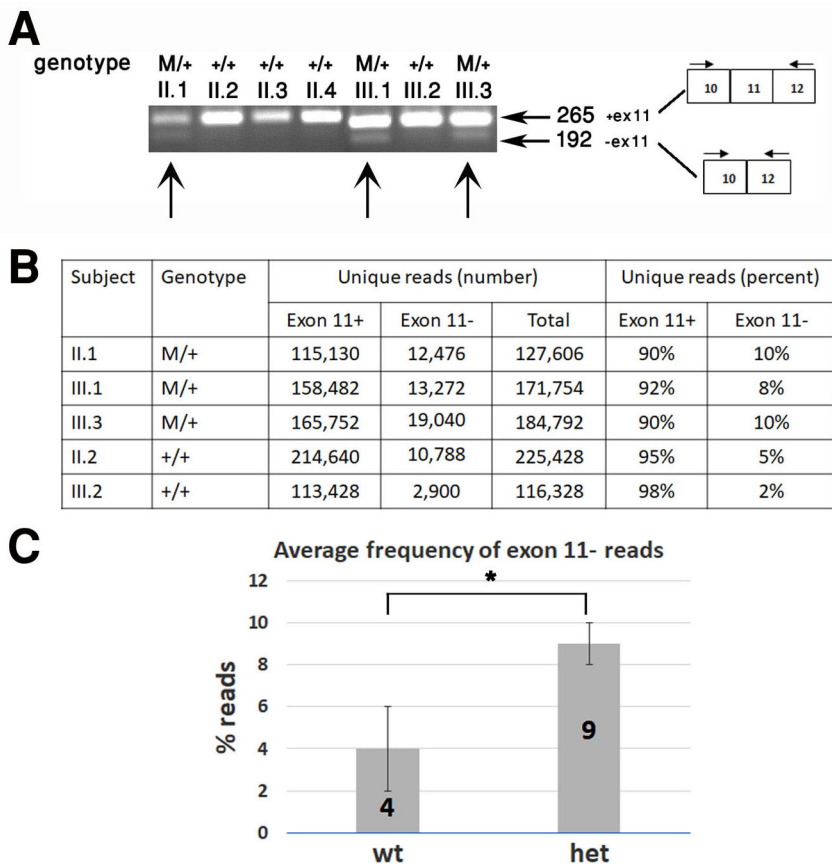


Figure 4. Evaluation of the effect of *PRPF31* c.1146+5G>T on splicing in vivo. **A:** RT-PCR analysis of a lymphocyte-derived RNA sample with primers in exons 10 and 12. The genotypes of the family members are indicated above each lane. **B:** Evaluation of the relative abundance of alternatively spliced transcripts using amplicon-based next-generation sequencing. Shown is the number and percentage of exon 11+ compared with those of exon 11- unique reads in each tested family member. **C:** Average frequency of exon 11- transcripts in the wt and heterozygous (het) individuals. +, wt; M, mutant. \*p < 0.05.

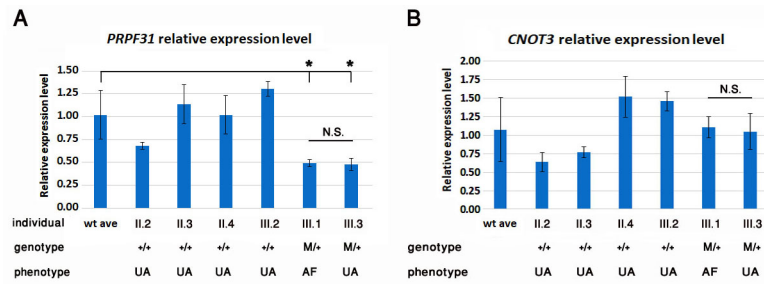


Figure 5. Relative expression levels of *PRPF31* and *CNOT3* in TB209 family members. The *PRPF31* (A) and *CNOT3* (B) expression levels in blood lymphocytes (measured in triplicate) were normalized to the housekeeping gene *GAPDH*. The error bars refer to the standard deviation of the mean for each individual. ave, average; +, wt; M, mutant; UA, unaffected; AF, affected, N.S., not significant. \* $p < 0.05$ .

years, it is unlikely that he was affected, although late onset of disease symptoms cannot be excluded.

One factor that affects the penetrance of *PRPF31* mutations is the expression level of the nonmutant *PRPF31* allele [6]. *CNOT3* negatively regulates the expression of *PRPF31*, and in some studies, the lymphoblasts of asymptomatic *PRPF31* mutation carriers were found to have higher *PRPF31* expression levels and lower *CNOT3* expression levels than those of symptomatic carriers [8,9]. Hence, we evaluated several factors that have been suggested to correlate with the non-penetrance of *PRPF31* mutations. One was the *CNOT3* rs4806718 single-nucleotide polymorphism (SNP; C/T). A correlation between the T allele of this polymorphism and non-penetrance was previously suggested [9]. In family TB209, the *CNOT3* rs4806718 genotype did not correlate with disease penetrance, as all three carriers of the *PRPF31* mutation, both symptomatic (subjects II:1 and III:1) and asymptomatic individuals (Subject III:3), were heterozygotes for this SNP. We also determined the number of cis-acting MSR1 elements adjacent to the *PRPF31* core promoter; four-copy repeats have been associated with non-penetrance [10,11]. In family TB209, no such correlation was found, as all family members, including the non-penetrant individual, were homozygous for the three-copy MSR1 repeat. We then evaluated the relative expression levels of *PRPF31* and *CNOT3* in lymphocyte samples from TB209 family members using qPCR. The PCR primers used for *PRPF31* amplification were located in exons 3 and 5, and therefore amplified all *PRPF31* transcripts, including both the wt and mutant. However, given the low abundance of exon 11- transcripts (Figure 4), most amplification products were expected to represent wt transcripts. The analysis revealed that subjects III:1 (symptomatic) and III:3 (asymptomatic) had similar and reduced expression levels of *PRPF31* (approximately 50% of the average expression level in the wt controls; Figure 5). The *CNOT3* expression level showed no statistically significant

difference between the two individuals and was similar to the average expression level in the wt controls (Figure 5). Finally, we genotyped the family members for three SNPs in the *PRPF31* gene to reconstruct the *PRPF31*-linked haplotype in chromosomes harboring the wt rather than the mutant allele. The analysis revealed that subjects III:1 and III:3 inherited different copies of chromosome 19 from their father (Appendix 2). These results support the presence of a genetic modifier leading to the non-penetrance in Subject III:3 in cis with *PRPF31*, although the effect of such a putative modifier on the *PRPF31* expression level was not apparent in the lymphocytes.

## DISCUSSION

The primary aim of the present study was to identify the molecular mechanism of adRP in an Israeli Muslim Arab family. Genetic analysis revealed a novel heterozygous intronic mutation of *PRPF31*, c.1146+5G>T. The affected individuals carrying this mutation had classic symptoms of RP with childhood onset. The clinical findings from these patients were similar to those reported previously in patients with other *PRPF31* mutations [3]. To evaluate the effect of c.1146+5G>T on splicing, we performed in vitro and in vivo splicing analyses. The results of the analyses indicated that some degree of alternative splicing of exon 11 is normal and that the c.1146+5G>T allele further weakens the intron 11 donor splice site and enhances the skipping of intron 11. At the protein level, skipping of exon 11 was expected to cause a frameshift that yields an aberrant truncated protein (p.Tyr359Serfs\*29). The presence of such a truncated protein was not confirmed experimentally. If it was indeed generated, it could be associated with either loss of function and/or a dominant negative effect [3]. Nevertheless, although exon 11- transcripts were more abundant in the individuals harboring the c.1146+5G>T allele than in the wt individuals, the relative frequency of these transcripts was low in both

groups. Moreover, the total *PRPF31* expression level in the carriers of the c.1146+5G>T allele was approximately half of the expression level in the wt individuals. These results indicate that the mutant transcript was probably unstable and may be subjected to the NMD mechanism and support haplo-insufficiency as the disease mechanism associated with the c.1146+5G>T mutation. In this context, it is of special interest to mention another *PRPF31* mutation, c.1115\_1125del. This mutation is located in exon 11 and can inactivate an exonic splicing enhancer and thus promote the skipping of exon 11 during mRNA splicing and result in an out-of-frame premature termination codon in exon 12, similar to the effect of c.1146+5G>T [14]. Exon 11- transcripts generated as a result of this mutation were shown to undergo degradation through the NMD mechanism [14].

One family member carried the c.1146+5G>T mutation with no phenotypic expression. This phenomenon has been previously reported in families segregating *PRPF31* mutations [3]. However, we could not identify the factors contributing to the reduced penetrance in this family. The *CNOT3* rs4806718 genotype did not correlate with disease penetrance in this family, which is in agreement with a previous study [10] that did not replicate the original observation made by Venturini et al. [9]. RP11 disease non-penetrance was also associated with the presence of a four-copy MSR1 repeat in the *PRPF31* promoter in many RP11 asymptomatic carriers [10,11]. In family TB209, all family members, including the asymptomatic carrier, were homozygous for the three-copy MSR1 repeat. *PRPF31* penetrance correlates, at least in part, with the expression level of the nonmutant *PRPF31* allele [6], which reversely correlated with the *CNOT3* expression level [8,9]. In family TB209, the asymptomatic carrier had a reduced *PRPF31* expression level, which was similar to the expression level in his affected brother. The *CNOT3* expression levels were similar in both individuals and the wt controls. However, these expression levels were measured in blood lymphocytes and may not reflect the expression levels in retinal photoreceptors. For example, in a study performed by McLenachan et al. [10], the *PRPF31* expression level of a non-penetrant carrier was not higher than that of symptomatic individuals when measured in skin fibroblasts but was an intermediate between wt and symptomatic individuals when measured in retinal organoid cultures (differentiated from induced pluripotent stem cells). It is possible that the asymptomatic carrier in family TB209 had an increased expression level of the wt *PRPF31* allele in his retina, which compensated for the mutant allele. Alternatively, the non-penetrance in this individual might have resulted from other genetic and/or environmental factors that are still to be determined.

In conclusion, this report expands the spectrum of pathogenic mutations in *PRPF31* and further demonstrates the importance of intronic mutations. Moreover, it demonstrates the phenomenon of incomplete penetrance, which was previously associated with *PRPF31* mutations. The fact that non-penetrance in the family in this study could not be explained by any of the known mechanisms suggests the possible contribution of a novel modifier of *PRPF31* penetrance.

## APPENDIX 1. PRIMERS USED IN THIS STUDY.

To access the data, click or select the words “[Appendix 1.](#)”

## APPENDIX 2. PRPF31-LINKED HAPLOTYPES IN FAMILY TB209.

To access the data, click or select the words “[Appendix 2.](#)” The haplotypes, represented by vertical bars, are composed of three single nucleotide polymorphisms (SNPs) flanking the c.1146+5G>T allele of the *PRPF31* gene, on chromosome 19q13.42. SNP order and genomic coordinates are indicated to the right. The c.1146+5G>T-bearing haplotype is marked in red. Paternal haplotypes (in brackets) were reconstructed based on genotypes of individuals 1, 5, 6 and 7, but not molecularly confirmed. Individuals 5 and 7 inherited different paternal chromosomes.

## ACKNOWLEDGMENTS

We are grateful to all family members for their participation in this study. We thank Elizabeta Ginzburg, Margalit Peleg and Liat Linde for amplicon-based NGS. This work was supported by research grant BR-GE-0518-0734 from the Foundation Fighting Blindness to TB, DS and EB.

## REFERENCES

1. Verbakel SK, van Huet RAC, Boon CJF, den Hollander AI, Collin RWJ, Klaver CCW, Hoyng CB, Roepman R, Klevering BJ. Non-syndromic retinitis pigmentosa. *Prog Retin Eye Res* 2018; 66:157-86. [PMID: 29597005].
2. Vithana EN, Abu-Safieh L, Allen MJ, Carey A, Papaioannou M, Chakarova C, Al-Magthteh M, Ebenezer ND, Willis C, Moore AT, Bird AC, Hunt DM, Bhattacharya SS. A human homolog of yeast pre-mRNA splicing gene, PRP31, underlies autosomal dominant retinitis pigmentosa on chromosome 19q13.4 (RP11). *Mol Cell* 2001; 8:375-81. [PMID: 11545739].
3. Whewey G, Douglas A, Baralle D, Guillot E. Mutation spectrum of PRPF31, genotype-phenotype correlation in retinitis pigmentosa, and opportunities for therapy. *Exp Eye Res* 2020; 192:107950-[PMID: 32014492].

4. Rose AM, Bhattacharya SS. Variant haploinsufficiency and phenotypic non-penetrance in PRPF31-associated retinitis pigmentosa. *Clin Genet* 2016; 90:118-26. [PMID: 26853529].
5. Valdes-Sanchez L, Calado SM, de la Cerda B, Aramburu A, Garcia-Delgado AB, Massalini S, Montero-Sanchez A, Bhatia V, Rodriguez-Bocanegra E, Diez-Lloret A, Rodriguez-Martinez D, Chakarova C, Bhattacharya SS, Diaz-Corrales FJ. Retinal pigment epithelium degeneration caused by aggregation of PRPF31 and the role of HSP70 family of proteins. *Mol Med* 2019; 26:1-[PMID: 31892304].
6. Rivolta C, McGee TL, Rio Frio T, Jensen RV, Berson EL, Dryja TP. Variation in retinitis pigmentosa-11 (PRPF31 or RP11) gene expression between symptomatic and asymptomatic patients with dominant RP11 mutations. *Hum Mutat* 2006; 27:644-53. [PMID: 16708387].
7. Rio Frio T, Civic N, Ransijn A, Beckmann JS, Rivolta C. Two trans-acting eQTLs modulate the penetrance of PRPF31 mutations. *Hum Mol Genet* 2008; 17:3154-65. [PMID: 18640990].
8. Rose AM, Shah AZ, Venturini G, Rivolta C, Rose GE, Bhattacharya SS. Dominant PRPF31 mutations are hypostatic to a recessive CNOT3 polymorphism in retinitis pigmentosa: a novel phenomenon of “linked trans-acting epistasis”. *Ann Hum Genet* 2014; 78:62-71. [PMID: 24116917].
9. Venturini G, Rose AM, Shah AZ, Bhattacharya SS, Rivolta C. CNOT3 is a modifier of PRPF31 mutations in retinitis pigmentosa with incomplete penetrance. *PLoS Genet* 2012; 8:e1003040-[PMID: 23144630].
10. McLenachan S, Zhang D, Grainok J, Zhang X, Huang Z, Chen SC, Zaw K, Lima A, Jennings L, Roshandel D, Moon SY, Heath Jeffery RC, Attia MS, Thompson JA, Lamey TM, McLaren TL, De Roach J, Fletcher S, Chen FK. Determinants of Disease Penetrance in PRPF31-Associated Retinopathy. *Genes (Basel)* 2021; 12:1542-[PMID: 34680937].
11. Rose AM, Shah AZ, Venturini G, Krishna A, Chakravarti A, Rivolta C, Bhattacharya SS. Transcriptional regulation of PRPF31 gene expression by MSR1 repeat elements causes incomplete penetrance in retinitis pigmentosa. *Sci Rep* 2016; 6:19450-[PMID: 26781568].
12. Grimberg J, Nawoschik S, Belluscio L, McKee R, Turck A, Eisenberg A. A simple and efficient non-organic procedure for the isolation of genomic DNA from blood. *Nucleic Acids Res* 1989; 17:8390-[PMID: 2813076].
13. Almeida JL, Hill CR, Cole KD. Authentication of African green monkey cell lines using human short tandem repeat markers. *BMC Biotechnol* 2011; 11:102-[PMID: 22059503].
14. Rio Frio T, Wade NM, Ransijn A, Berson EL, Beckmann JS, Rivolta C. Premature termination codons in PRPF31 cause retinitis pigmentosa via haploinsufficiency due to nonsense-mediated mRNA decay. *J Clin Invest* 2008; 118:1519-31. [PMID: 18317597].

Articles are provided courtesy of Emory University and the Zhongshan Ophthalmic Center, Sun Yat-sen University, P.R. China. The print version of this article was created on 6 October 2022. This reflects all typographical corrections and errata to the article through that date. Details of any changes may be found in the online version of the article.